

Broadband spin dynamics of the magnetic vortex state: Effect of the pulsed field direction

Xiaobin Zhu and Zhigang Liu

Department of Physics, University of Alberta, Edmonton, Alberta Canada, T6G 2J1

Vitali Metlushko

Department of Electrical and Computer Engineering, University of Illinois at Chicago, Chicago, Illinois 60607, USA

Peter Grütter

Department of Physics, McGill University, Montreal, Quebec, Canada, H3A 3T8

Mark R. Freeman

Department of Physics, University of Alberta, Edmonton, Alberta, Canada, T6G 2J1

(Received 7 January 2005; published 27 May 2005)

The dynamic spin modes observed in magnetic vortex structures are shown to depend strongly on the nature of the initial excitation by a transient pulse field. In submicrometer-sized Permalloy disks, when a uniform perpendicular transient field is used to perturb the magnetization, radial standing-wave modes are excited; whereas if an in-plane transient field is used, angular or azimuthal modes are formed. The existence of the vortex core is responsible for a frequency splitting of the azimuthal modes, as demonstrated through comparison to micromagnetic simulations of a ring geometry.

DOI: 10.1103/PhysRevB.71.180408

PACS number(s): 75.40.Gb, 76.50.+g, 75.60.-d

The magnetic vortex is often found to be the ground state in micrometer and submicrometer-scale soft magnetic disks.¹⁻⁴ The spin dynamics of the vortex state has drawn increasing attention due to fundamental interest and to its close relation to questions of high-speed magnetization dynamics.⁵⁻¹³ In this state, the static magnetization pattern is circular about the disk center, while in the core, the magnetization is perpendicular to the disk. The theoretical prediction of the magnetic normal modes of the vortex state is still a challenge owing to the difficulty of analytic calculation, despite the well-defined symmetry of the state.^{10,13} Simplified models predict that spin dynamics in the vortex can be described by discrete spin-wave spectrum with modes with integral numbers, m and n , which represent the azimuthal and radial modes.^{6,13} If standing wave patterns are formed, m and n represent the number of nodes in the angular and radial direction. These modes could also be coupled with one another.¹³

The purpose of the present paper is to investigate the identification and selection of detectable precessional modes. Both Brillouin light scattering¹³ (BLS) and pulsed ferromagnetic resonance⁵ (FMR) previously have been used to study the spin dynamics in vortex state.^{7,11,12} In the pulse FMR technique, an ultrafast magnetic field tips the sample's magnetization away from its equilibrium configuration, and the resulting magnetization response is monitored stroboscopically.^{5,7} Different excitation modes have been observed for various sized disks. The gyrotropic mode,^{11,14} together with up to two modes at higher resonance frequency have been reported by the Minnesota group.¹¹ In the Regensburg group, several precessional modes were observed in micrometer-sized structures.¹² It is still not clear, however, how the transient field selects the spin modes. In this paper, we study the spin dynamics of nominally identical submicrometer diameter disks exposed to different transient field

directions. The results of pulsed FMR measurements are compared to micromagnetic modeling.

An array of 30-nm-thick, 700-nm-diam Permalloy disks at 2- μm center-to-center spacing was prepared on a 100-nm-thick SiN membrane using electron beam lithography. For comparative studies, different sized disks having diameters from 200 nm to 1 μm were prepared on a silicon substrate. At remanence, these disks are in the vortex state, as has been examined by magnetic force microscopy (MFM).⁴ Figure 1(a) shows a MFM image of a 500-nm-sized disk. The polarity of the vortex core is also identified, as it is (in this case) repulsive to the stray field from the MFM tip, shown by the black dot at the image center.

Figure 1(b) shows a schematic of the setup for broadband FMR. The transient field that drives the magnetization away from equilibrium is produced using the photoconductive switch technique.¹⁵ The resulting dynamic process is probed via the magneto-optical Kerr effect at a variable time delay. The disk array is placed on top of a coplanar transmission line with the sample surface facing the lithographic stripline. The width of the wires is 20 μm , with a 20- μm spacing. The current pulse applies simultaneously a perpendicular transient field to disks located between the wires, and an in-plane transient field to those on top of a wire (with a small perpendicular component produced by the neighboring wire). By varying the probe beam position, the effects of transient field direction could be investigated. The focus spot size of the probe beam through 100-nm SiN membrane is about 500 nm, small enough to study individual disks.

Typical time-domain FMR curves for orthogonal directions of the transient field excitation are shown in Figs. 1(c) and 1(d). Periodic oscillations with gradually decreasing amplitude are observed for the transient excitation perpendicular to the disk, with an early response that also reflects the pulse profile. High frequency modes superimposed upon a very low frequency oscillation are observed for the pulse

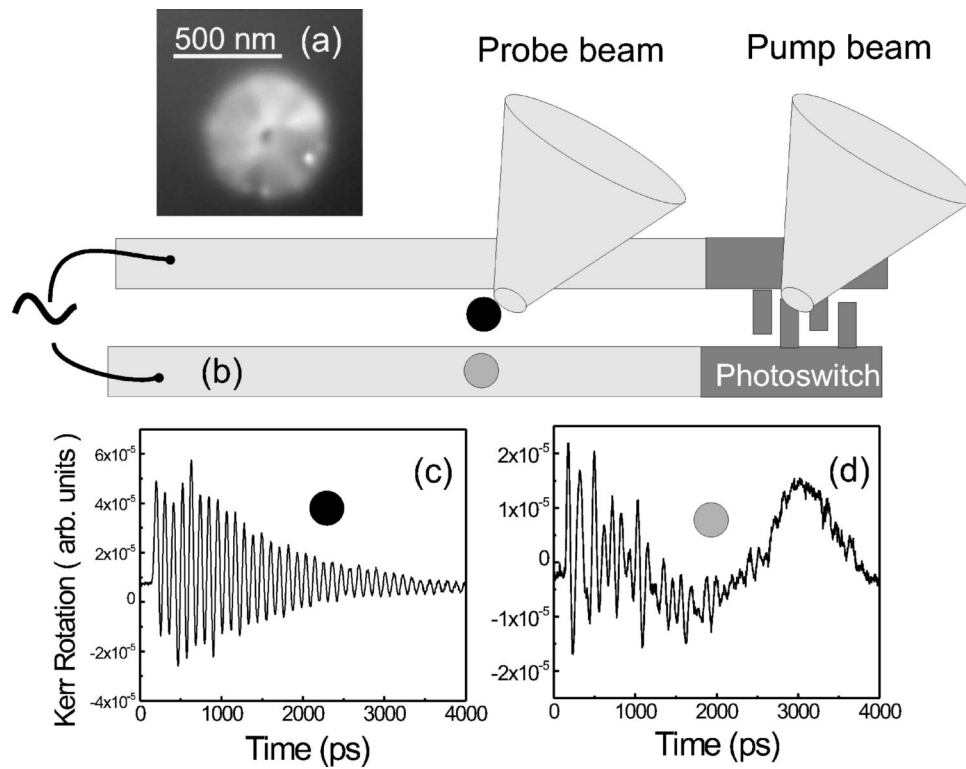


FIG. 1. The sample geometry, and broadband ferromagnetic resonance oscillations of Permalloy disks in the vortex state. (a) MFM image of a 500-nm-diam Permalloy disk. (b) Schematic drawing of the experimental setup (not to scale). The pump beam from a femtosecond Ti:Sapphire oscillator launches picosecond current pulses. The resulting ultrafast magnetic field drives small amplitude precessional motion of the magnetization. The magnetization change is measured in the time domain using the polar Kerr effect with a controlled delay between the pump and probe beam pulses. (c) and (d) Time-domain FMR curves of individual 700-nm-sized Permalloy disks for ultrafast magnetic field applied perpendicular to the disk [between the wires, at the position of the center of the black dot, (c)] and parallel to the disk [on top of a wire, at the position of the center of the gray dot (d)]. The widths of, and the space between, the stripe lines are all 20 μm . The dark gray area: photoswitch lithographically patterned on the GaAs substrate. The black and gray dots roughly demarcate the regions of perpendicular and parallel excitation, respectively.

field mainly parallel to the disk, as shown in Fig. 1(d). This curve is very similar to the results obtained from a purely in-plane pulse excitation.¹¹

The effect of the transient field direction is rendered in the frequency domain through Fourier transformation of the temporal traces, as shown in Fig. 2. For the perpendicular transient field excitation, a 9.3-GHz resonance dominates all others with its high spectrum amplitude. Besides this frequency, there are two additional resonances, at 2.4 GHz and at 13 GHz, each with a small amplitude. In contrast, the frequency spectrum from the in-plane field pulse shows multiple peaks of comparable amplitude at frequencies 0.4, 6, 7.25, and 9.5 GHz, with weaker signatures at 10.7 and 11.6 GHz, and a broader feature at 12.8 GHz.

Since the dimensions of a disk (700 nm) are very small in comparison with those of the stripline (20 μm), the pulse field generated at the disk is very homogeneous. When a perpendicular pulse is applied, all of the magnetization outside the core experiences the same magnitude of initial torque. The magnetization precesses uniformly (with the exception of the vortex core). The 9.3 GHz resonance frequency of the vortex state in response to a perpendicular pulse excitation may be obtained as a solution to the Larmor precession equation, which yields

$$f_{\text{th}} = \frac{1}{2\pi} \gamma M_s \sqrt{N_\rho N_z}, \quad (1)$$

where N_ρ and N_z are the demagnetizing factors in the radial and perpendicular directions.⁷ The demagnetizing factor in the angular direction is zero in this case due to the circulation of magnetization. As this mode has no nodes in the radial direction between the center and the edge, and none in the angular direction, it is assigned the mode number (0,0). The higher frequency resonance at 13 GHz represents a mode with a radial node.^{12,13} From the simulation results presented below, we find that this oscillation corresponds to the radial mode with $n=2$. The mode at 2.4 GHz is possibly an edge localized mode.¹⁶ However, further studies with better spatial resolution are required to clarify this.

For in-plane pulsed excitation, the torque on the core in combination with the now nonuniform torque on the circulating magnetization causes an initial push of the vortex core away from the center, followed by a gyrotropic motion about the center of the off-centered vortex. The gyrotropic frequency for the investigated disk is found to be 0.44 GHz, shown in Fig. 2. This value is consistent with theoretical expectation,^{8,17} and agrees with the results obtained in other groups.^{11,14} This mode is not observed with perpendicular

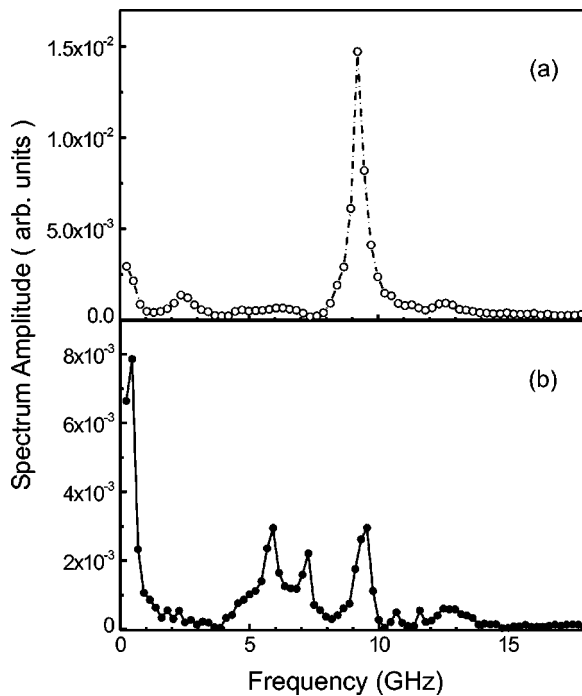


FIG. 2. Fourier transforms of the experimental time-domain ferromagnetic resonance curves. The dashed line (open circles) shows the spectrum for perpendicular pulse field excitation; the solid line (filled circles) is from the in-plane pulse field excitation.

pulse excitation as the vortex core position is not affected by the perpendicular transient field.

The inhomogeneous antisymmetric initial torque on the vortex state magnetization produced by the in-plane pulse excites the magnetic normal modes with rotational symmetry, seen here at the frequencies of 6.0 and 7.25 GHz. The higher frequency modes at 9.5 and 12.8 GHz, are the same modes as found with perpendicular excitation. Measuring individual disks, the disk-to-disk frequency variation is found to be about 0.2 GHz (both for in-plane and out-of-plane excitation).

In order to understand the observed spin dynamic behavior, and to identify these modes, micromagnetic modeling was conducted using a commercial code.¹⁸

The total magneto-optical signal from a given mode is determined by the spatial average of the magnetization change under the probe spot. This is very small when nearly equal local regions precess with the opposite phase. In Fig. 3, we plot the magnetization change of a half disk as a function of time. This approximates the experimental conditions of Figs. 1(c) and 1(d) for perpendicular and in-plane excitations, but is not an exact match to the experimental conditions. The resonance frequencies are obtained through Fourier transformation. Figs. 3(c)–3(e) plot the amplitude spectra of the simulation results (averaged through the half disk) as a function of frequency for the transient field pulse applied perpendicular to the disk (c), parallel to the disk plane (d), and in plane for the wide ring (e). For perpendicular pulse field excitation, a dominant resonance frequency at 9.7 GHz appears, with weak satellite peaks at 12 and 13 GHz. For the in-plane pulse excitation, the simulations yield resonance

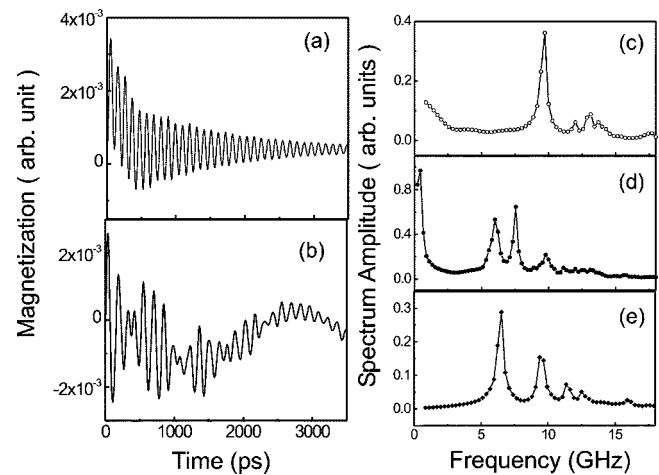


FIG. 3. Time-domain ferromagnetic resonance curves from micromagnetic simulation. FMR curve for pulsed magnetic field applied (a) perpendicular to the disk, and (b) parallel to the disk. (c)–(e) The spectrum amplitude as a function of frequency for the transient field applied (c) perpendicular to the disk, (d) parallel to the disk. (e) The simulation for the transient field in the plane of a wide ring (same outer diameter as the disk, with a 5-nm-diam central hole).

peaks at 0.44, 6.0, 7.5, 9.7, 11, 12, 12.5, and 13 GHz. These results reproduce the experimental observations reasonably well.

From the simulation results, we find that the precessional motion at 9.7 GHz is nearly uniform across the disk, outside the vortex core. At 13 GHz, there are two nodes in the radial direction,¹² and a phase plot from the Fourier transform shows a 180-degree phase change across each node. For the 12-GHz mode, there is one node in the radial direction. The uniform field excitation and spatially averaged detection both make these modes appear much weaker than the uniform mode.

For the in-plane pulse field excitation, we see the gyrotropic mode, as well as a 9.7-GHz peak indicating that the uniform mode (0,0) is also excited. The higher frequency modes (above 9.7 GHz) are also manifest. Of greatest interest here, however, are the new modes at resonance frequencies below the uniform mode, with relatively large amplitude. The spatial profiles of the amplitudes for 6.0 and 7.5 GHz are nearly rotationally symmetric. Radially, the amplitude is largest close to the center, and gradually decreases toward the disk boundary. The phase changes continuously in the angular direction, indicating that instead of having standing nodes these modes are traveling waves in the angular direction, like the circularly polarized modes observed by the Regensburg group.¹²

Schematic illustrations of the instantaneous phase configuration of the left- and right-circularly polarized modes are shown in the left-hand column of Fig. 4. To further elucidate these modes, we reconstruct time-domain configurations based on the amplitudes and phases of the oscillations at these frequencies. Panels 4(a)–4(d) show a few frames of the 6.0-GHz mode. This mode is an angular mode with $|m| = 1$, as the phase change is 2π around a complete rotation. The spatially antisymmetric torque from the in-plane excita-

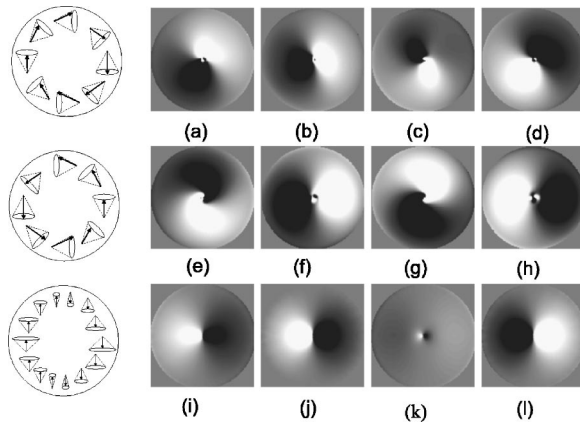


FIG. 4. On the left side of each row, a schematic of the instantaneous positions of local magnetization is shown, indicating the relative amplitude and phase of the precession. The gray scale portraits show the reconstructed out-of-plane magnetization component change at select times after the onset of the excitation pulse, for the different resonance frequencies (black and white represent positive and negative change with respect to the initial state, where the magnetization is entirely in plane away from the core). The panels (a)–(h) are for a 700-nm diam Permalloy disk; (i)–(l) are for a wide ring with the same outer diameter as the disk and a 5-nm-diam hole. Panels (a)–(d) show the 6-GHz mode of the disk; (e)–(h) the 7.5-GHz mode; and (i)–(l) the 6.7-GHz mode of the ring. The times are: 10 ps (a),(e),(i); 40 ps (b),(e),(j); 70 ps (c),(g),(k); and 100 ps (d),(h),(l).

tion pulse couples to this mode directly. The slow gyrotropic motion of the vortex ensures the traveling nature of this mode: in a quasistatic limit of the gyrotropic motion, the high frequency modes would adiabatically follow the inhomogeneous magnetization profile of the moving vortex core. Panels 4(e)–4(h) show snapshots at the same times as Figs. 4(a)–4(d), but for the frequency of 7.5 GHz. This mode circulates with the opposite helicity of the 6.0-GHz mode, and also has an angular mode number of $|m|=1$. The frequency splitting of these modes has been discussed theoretically.^{6,10} The perpendicular magnetization of the vortex core breaks the otherwise perfect symmetry for left- and right-handed rotations. The frequency splitting arises from the fact that the magnon scattering by the vortex core is different for the clockwise and anticlockwise modes.¹⁰ The frequency difference between the $|m|=1$ modes can be larger than twice the

gyrotropic frequency of the vortex core.⁶ Given that the frequency of the gyrotropic mode is 0.44 GHz in the present case, the frequency splitting of around 1.5 GHz for $|m|=1$ is reasonable, although detailed analytic calculation is still a challenge.

For comparison, we also simulate a wide ring structure corresponding to a disk of the same size with a central hole of 5-nm diam to eliminate the vortex core. Only one resonance frequency is found in the range of 6–8 GHz, as shown in Fig. 3(c), at a frequency of 6.6 ± 0.1 GHz. Without the vortex core, the clockwise and anticlockwise angular modes are degenerate. As a result, the mode oscillates as a standing wave polarized along the transient field direction. The reconstructed time-domain magnetization change of this mode is shown in panels Figs. 4(i)–4(l), with a corresponding schematic of the instantaneous local precession cones to the left of the row.

The magnitude of the splitting and of the vortex core gyrotropic frequency depend on the disk radius (R) and film thickness (t) according to t/R^α with $\alpha=1$ or 2 .^{6,8,10} For diameters of several micrometers or larger, at thicknesses on the order of 30 nm, the frequency splitting is usually less than 0.1 GHz. This is near the typical frequency resolution of the optical pump-probe measurement, as the resolution is limited by the maximum optical delay time and by the damping constant of the magnetic material. This could explain why the angular standing wave mode formed in large disks (6 μm) in Ref. 12.

In summary, a subset of the predicted magnetic normal modes of submicrometer disks in the magnetic vortex state have been observed experimentally. In pump-probe measurements, the detectable modes are dictated by how the excitation pulse couples to the magnetic modes. For perpendicular pulsed field, the uniform mode (0,0) is strongly excited, and some higher frequency modes with radial nodes are weakly visible. For in-plane pulsed excitation, the $|m|=1$ modes are well matched to the antisymmetric torque profile of the transient field. These modes have a substantial frequency splitting and are circularly polarized, due to the presence and motion of the vortex core.

The work at the University of Alberta was supported by NSERC, CIAR, iCORE, and Alberta Ingenuity. The work at UIC was supported by NSF Grants No. ECS-0202780 and DMR-0210519M (V.M.). The authors are also thankful to Fabrizio Nizzoli for useful discussions.

¹T. Shinjo *et al.*, *Science* **289**, 930 (2000).

²R. P. Cowburn *et al.*, *Phys. Rev. Lett.* **83**, 1042 (1999).

³A. Wachowiak *et al.*, *Science* **298**, 577 (2002).

⁴X. Zhu *et al.*, *Appl. Phys. Lett.* **80**, 4789 (2002).

⁵W. K. Hiebert *et al.*, *Phys. Rev. Lett.* **79**, 1134 (1997).

⁶B. A. Ivanov *et al.*, *Phys. Rev. B* **58**, 8464 (1998).

⁷Y. Acremann *et al.*, *Science* **290**, 492 (2000).

⁸K. Yu. Guslienko *et al.*, *J. Appl. Phys.* **91**, 8037 (2002).

⁹V. Novosad *et al.*, *Phys. Rev. B* **66**, 052407 (2002).

¹⁰B. A. Ivanov and C. E. Zaspel, *Appl. Phys. Lett.* **81**, 1261 (2002).

¹¹J. P. Park *et al.*, *Phys. Rev. B* **67**, 020403(R) (2003).

¹²M. Buess *et al.*, *Phys. Rev. Lett.* **93**, 077207 (2004).

¹³L. Giovannini *et al.*, *Phys. Rev. B* **70**, 172404 (2004).

¹⁴S.-B. Choe *et al.*, *Science* **304**, 420 (2004).

¹⁵M. R. Freeman *et al.*, *IEEE Trans. Magn.* **27**, 4840 (1991).

¹⁶C. Bayer *et al.*, *Phys. Rev. B* **69**, 134401 (2004).

¹⁷B. A. Ivanov and C. E. Zaspel, *J. Appl. Phys.* **95**, 7444 (2004).

¹⁸LLG Micromagnetics Simulator, llgmicro@mindsping.com. The cell size is $2.5 \times 2.5 \times 5$ nm. The pulse fields for simulation have a 10-ps rise time, 200-ps decay time, with the peak value of 1.6 kA/m.